Trop J Nat Prod Res, April 2026; 10(4): 8877 – 8886

ISSN 2616-0684 (Print)
ISSN 2616-0692 (Electronic)

Tropical Journal of Natural Product Research

Available online at https://www.tjnpr.org

Original Research Article

Centella asiatica Extract and Arbutin Hybrid Nanoemulsion as a Synergistic Inhibitor of Melanogenesis

Safri S. Wibowo[1], Yosef A. Christian[1], Adi Hermawansyah[2], Rini Dwiastuti[1], Agustina Setiawati[1]*

[1]Faculty of Pharmacy, Sanata Dharma University, Paingan, Maguwoharjo, Depok, Sleman, Yogyakarta, 55282, Indonesia
[2]*Faculty of Medicine and Health Sciences, University of Muhammadiyah Yogyakarta, Kasihan, Bantul, Yogyakarta 55183, Indonesia*

ARTICLE INFO

Article history:
Received 10 November 2025
Revised 16 February 2026
Accepted 02 April 2026
Published online 01 May 2026

ABSTRACT

Melanogenesis is the molecular process that produces melanin pigment in melanocytes. One of the well-known commercial anti-melanogenic agents is *β*-arbutin, which lacks stability and skin penetration. Previous studies combined *β*-arbutin and asiaticoside, a triterpenoid glycoside from *Centella asiatica*, to enhance antioxidant and antimelanogenic properties. This study aimed to formulate a hybrid nanoemulsion of *β*-arbutin and *C. asiatica* extract for synergistic inhibition of melanogenesis, supported by bioinformatics and molecular docking validation. Bioinformatics analysis was conducted to identify the gene targets of *β*-arbutin and asiaticoside in melanogenesis. The interaction of the compounds with tyrosinase (TYR) was examined through molecular docking. Before formulation, the extracts were identified for asiaticoside using thin-layer chromatography (TLC). Then, hybrid nanoemulsions of *β*-arbutin and asiaticoside combination were formulated and characterized for physicochemical stability and tested for tyrosinase inhibition and melanin suppression in B16F10 melanoma cells. TYR, Microphthalmia-associated Transcription Factor (MITF), and Dopachrome Tautomerase (DCT) were identified as major target genes that had strong binding affinities with TYR for asiaticoside (−6.38 kcal/mol) and *β*-arbutin (−6.23 kcal/mol). The optimized hybrid nanoemulsion (Fae) exhibited nanosized droplets (10.44 ± 0.28 nm), low polydispersity index PDI (<0.2), and high tyrosinase inhibition (91.54 ± 0.77%). Fae significantly reduced intracellular melanin production (13.08 ± 2.02%) compared to single formulations. This indicates that the *β*-arbutin and *Centella asiatica* hybrid nanoemulsion enhances TYR enzyme inhibition and cellular anti-melanogenic activity, presenting a promising natural-based approach for topical skin lightening and hyperpigmentation therapy.

Keywords: Arbutin, Asiaticoside, Bioinformatics, Hyperpigmentation, Molecular docking, Skin lightening

Introduction

Hyperpigmentation is one of the aesthetic problems of human skin, characterized by post-inflammatory hyperpigmentation, melasma, solar lentigo, age spots, and freckles, caused by overproduction and accumulation of melanin or an elevated number of melanocytes producing melanin within skin layers.[1,2] Melanogenesis is the molecular pathway of melanocytes, which are mostly found in the basal layer of the skin epidermis, to produce melanin pigment.[3] Melanin synthesis in the melanosome is regulated by key enzymes, namely tyrosinase (TYR), tyrosinase-related protein-1 (TRP-1), and tyrosinase-related protein-2 (TRP-2)[3] which is also known as dopachrome tautomerase (DCT).[4,5] Since TYR is the main enzyme in melanin biosynthesis, its inhibitors have gained great attention as commercial anti-hyperpigmentation agents in the cosmetics industry. Natural anti-tyrosinase compounds have recently attracted growing interest due to their lower toxicity and excellent bioavailability. Among these, plant-derived phenolic compounds represented one of the most abundant sources of tyrosinase inhibitors.[6]

***Corresponding author. E mail: nina@usd.ac.id
Tel: +62-(274)-883037

Citation: Wibowo SS, Christian YA, Hermawansyah A, Dwiastuti R, Setiawati A. *Centella asiatica* Extract and Arbutin Hybrid Nanoemulsion as a Synergistic Inhibitor of Melanogenesis. Trop J Nat Prod Res. 2025; 10(4): 8877 – 8886 https://doi.org/10.26538/tjnpr/v10i4.73

Official Journal of Natural Product Research Group, Faculty of Pharmacy, University of Benin, Benin City, Nigeria

Arbutin (4-hydroxyphenyl-*β*-D-glucopyranoside) is a naturally occurring compound found in various species of plants, as well as synthetic sources that include enzymatic processes and microorganisms' metabolite engineering.[7] It is widely applied for its skin-lightening properties and has been extensively used as a natural agent to inhibit melanin production.[7,8,9] Since arbutin has a hydroquinone moiety, it has the same activity as anti-hyperpigmentation, inhibiting tyrosinase and DOPAchrome to 5,6-dihydroxy-indole-2-carboxylic acid (DHICA) polymerase activity.[7-10] Arbutin is a hydrophilic polyphenol with two isomers, namely α-arbutin (4-hydroxyphenyl-*α*-glucopyranoside) and *β*-arbutin (4-hydroxyphenyl-β-glucopyranoside).[11] *β*-arbutin exhibited stronger inhibitory activity on melanogenesis and tyrosinase expression in B16-4A5 mouse melanoma cells compared to *α*-arbutin and kojic acid.[9] Despite its strong anti-melanogenic properties *in vitro*, its instability and potential to release hydroquinone limit its application in hyperpigmentation treatment, which raises safety concerns.[12] Many strategies have been developed to overcome these drawbacks. Formulation-based approaches, such as encapsulation in liposomes, nanoemulsions, or polymeric nanoparticles, improve β-arbutin's skin penetration and successfully protect it from degradation caused by light, heat, and pH variations.[13] Furthermore, *β*-arbutin presented a synergistic depigmenting effect at lower dosages when used with other non-toxic tyrosinase inhibitors, both synthetic and natural-based compounds, lowering the risk of adverse effects.[14,15,16] Recent studies suggest that combining *β*-arbutin with natural product-derived tyrosinase inhibitors produces synergistic depigmentation effects while limiting cytotoxicity. One of the phytochemical compounds reported to suppress melanogenesis is asiaticoside, a major compound in *Centella asiatica*. Asiaticoside exerted its anti-melanogenic effect mainly by downregulating tyrosinase expression and interfering with the

ISSN 2616-0684 (Print)
ISSN 2616-0692 (Electronic)

Microphthalmia-associated Transcription Factor (MITF) signaling pathway, resulting reducing melanin synthesis at both enzymatic and transcriptional levels. Furthermore, asiaticoside also exhibited strong antioxidant and anti-inflammatory properties, which mitigate oxidative stress induced pigmentation.[17-20] Our previous study demonstrated that an asiaticoside-rich fraction from *Centella asiatica* presented a strong *in vitro* tyrosinase inhibition activity.[21] Thus, the asiaticoside and *β*-arbutin combined formulation represented a promising strategy to enhance depigmenting efficacy while minimizing safety concerns.[8,11,12] *β*-arbutin primarily inhibited the catalytic activity of tyrosinase, whereas asiaticoside modulated melanogenesis and provided oxidative damage as cellular protection[21]. Therefore, their co-application may produce synergistic inhibition of melanogenesis through multi-target regulation, offering a more balanced and biocompatible approach to hyperpigmentation therapy.

The study attempts to formulate a depigmenting nanoemulsion incorporating *β*-arbutin and asiaticoside to prevent melanogenesis through multiple molecular targets in the melanogenesis pathway. A preliminary bioinformatics investigation was employed to identify potential gene/protein targets of *β*-arbutin and *Centella asiatica* extract in melanogenesis inhibition. This hybrid combination strategy is intended to enhance depigmenting efficacy at lower individual concentrations, suppressing possible cytotoxicity, and enhancing safety over single-compound therapies. However, both *β*-arbutin and asiaticoside exhibit low chemical stability and skin penetration, which limits their bioavailability in topical preparations. To tackle these challenges, this study designs a nanoemulsion-based delivery system to improve the solubility, physicochemical stability, and skin permeation of both active constituents. Nanoemulsions, characterized by their droplet size below 200 nm, improves the efficient transport of both lipophilic and hydrophilic molecules across the epidermal barrier.[22-25]

The novelty of this study lies in a hybrid formulation of *β*-arbutin–asiaticoside nanoemulsion, which has not been reported based on preliminary bioinformatics and molecular docking analysis. Accordingly, the formulation of a *β*-arbutin–asiaticoside nanoemulsion represents a safe and innovative therapeutic approach for hyperpigmentation. The effectiveness of this hybrid nanoemulsion of *β*-arbutin and asiaticoside in suppressing melanogenesis is investigated through *in vitro* tyrosinase assay and melanin synthesis inhibition of the nanoemulsion using murine melanoma B16F10 cells.

Materials and methods

Reagents and Chemicals:

The ethanol used for extraction was technical grade, whereas for TLC analysis, the stationary phase was silica gel GF_{254} (Sigma-Aldrich 1.05554.0001). The mobile phases used in this study were pro-analyst grade chloroform (1.02445.2500) and methanol (1.06007.2500), which were supplied by Sigma-Aldrich. Olive oil, Span, and Tween for the nanoemulsion formulation were pharmaceutical grade and obtained from Brataco Chemicals. Meanwhile, the pharmaceutical grade *β*-arbutin was provided by PT. Genero Pharmaceuticals. The micro well plates, tips, and e-tubes were purchased from Biologix. For the tyrosinase inhibition assay, the tyrosinase enzyme (Sigma-Aldrich, T3824-50KU), L-DOPA (Sigma-Aldrich, D9628), kojic acid (Sigma-Aldrich, K312), and phosphate-buffered saline (PBS) (Sigma-Aldrich P4417) were used. The B16F10 murine melanoma cell line was obtained from the European Collection of Authenticated Cell Culture (ECACC) (94042254). Then, Dulbecco's Modified Eagle Medium (DMEM) (Gibco, 11995-065), Fetal Bovine Serum (FBS) (Gibco, F7524), trypsin-EDTA (Gibco, 25200056), and penicillin-streptomycin (Gibco,15140) were also utilized.

Plant Collection and Identification

Centella asiatica herb was obtained from the Center for Research and Development of Medicinal Plants and Traditional Medicine (B2P2TOOT), Tawangmangu, Central Java, Indonesia (7.66479° S, 111.17982° E) on January 20, 2025. The authenticated herb was preserved as a voucher specimen number FF USD 010623. The herb was identified by Dr. Yohanes Dwiatmaka (Pharmacognosy and Phytochemistry Laboratory, Faculty of Pharmacy, Sanata Dharma University) with authentication number 01/LKTO/Far-USD/VI/2023, and the herbarium was kept in the same laboratory under the code 01062023FF.

Data Mining and Collection

This study was approved by the Faculty of Health Sciences, Respati University of Yogyakarta, with approval no. 96.3/FIKES/PL/XI/2025. Before the analysis, data on the crucial proteins and genes involved in melanogenesis and hyperpigmentation mechanisms were retrieved from public databases, including OMIM (www.omim.org), PubMed (www.ncbi.nlm.nih.gov), and GeneCard (www.genecard.org). The direct and indirect targets of asiaticoside and *β*-arbutin were screened using the STITCH database (www.stitch.embl.de). Specific proteins and genes in the pigmentation mechanism affected by asiaticoside and *β*-arbutin were identified using an interactive Venn diagram tool (http://www.interactivenn.net/).

Protein-Protein Interaction Network and Gene Clustering

Mapping the dynamic and complex interactions between various target proteins was performed in the Protein-protein interaction (PPI) network and gene clusterings. All target protein interactions were obtained using STRING-DB v11.5 (https://string-db.org), which served as the basis for the PPI network. Subsequently, gene analysis was conducted using Cytoscape 3.10.1 (https://cytoscape.org/). This study also used the Maximal Clique Centrality (MCC) algorithm of the Cyto-Hubba plugin to identify the top 3 genes with the top correlation in the PPI network. These genes were observed as hub genes related to pigmentation. In these processes, all bioinformatics analysis was performed on a system equipped with an 11th Gen Intel(R) Core (TM) i5-1155G7 @ 2.50GHz (2.50 GHz) processor.

In silico Molecular Docking

The TYR protein structure (PDB ID: 5M8O) and MITF (PDB ID: 7D8S) were obtained from the RCSB website (www.rcsb.org). Ligands were prepared using software BIOVIA Discovery Studio 2021. A native ligand was used as a control, followed by redocking with asiaticoside and *β*-arbutin. The ligands were protonated using Gasteiger charges, with Kollman charges applied to the macromolecule using AutodockTools 1.5.7. Molecular docking was conducted using a genetic algorithm with 200 GA runs. For the TYR complex with asiaticoside and TYR with *β*-arbutin, the ligands were placed at coordinates of x=-13.194, y=2.661, and z=-24.972, with a grid box size of 70 x 70 x 70 and a distance of 0.375 Å. For the MITF complex with asiaticoside and *β*-arbutin, the ligands were placed at coordinates of x=12.566, y=2.803, and z=5.125, with a grid box size of 70 x 70 and a distance of 0.375 Å. Control and cross-docking experiments were conducted under identical conditions. The resulting complexes were then visualized in both two-dimensional (2D) and three-dimensional (3D) structures after docking using BIOVIA Discovery Studio 2021. Docking accuracy was evaluated using the Root Mean Square Deviation (RMSD), with values $\leq$ 2.0 Å considered acceptable. The docking results were then employed to investigate the binding energies and protein-ligand interactions.

Extraction

Centella asiatica herb powder (60 mesh, 50 g) was macerated in 70% (v/v) ethanol for 24 h with shaking at 150 rpm. After 24 h, the mixture was filtered through a Buchner funnel, and the residue was subsequently subjected to remaceration three times under the same condition. The combined filtrates from all maceration steps were concentrated using a rotary evaporator at 15ºC and 10 mbar. The viscous extract was transferred to a pre-weighed porcelain dish, dried to a constant weight, and the percentage yield of the dried extract was calculated relative to the initial weight of the dried *Centella asiatica* material, resulting in a yield of 18-25%, and stored until further use in the next experiments.

Thin Layer Chromatography (TLC)

The *Centella asiatica* extract was investigated for asiaticoside content by Thin Layer Chromatography (TLC). The separation was carried out on silica gel GF254 pre-activated at 110 °C for 30 minutes, with hexane-ethyl acetate-diethylamine (80:20:2 v/v) as the mobile phase. Aliquots of 5 µL from both the sample and standard solutions were dropped onto the plates, eluted, and observed under UV light at 366 nm (CAMAG, Switzerland). The retention factor (R_f) values were then compared to confirm the presence of asiaticoside.[26]

Hybrid Nanoemulsion Formulation and Characterization

Three nanoemulsion formulations were prepared based on the formulation listed in the study,[27] namely Fa, Fe, and Fae, with different active components. Formulation Fa contained β-arbutin at a concentration of 140 ppm, while formulation Fe contained *Centella asiatica* extract at 240 ppm. Formulation Fae combined both active ingredients, consisting of *Centella asiatica* extract (240 ppm) and β-arbutin (140 ppm). All formulations used olive oil (0.5 g) as the oil phase, Tween 80 (7 g) as the surfactant, and propylene glycol (1 g) as the co-surfactant. Distilled water was added in sufficient quantity to obtain a final volume of 60 mL. Olive oil, serving as the oil phase, was mixed in a beaker with propylene glycol and rigorously stirred at 1000 rpm at 70 °C. Tween 60 was subsequently added, and the stirring continued for an additional 10 minutes. The *Centella asiatica* extract was dissolved in preheated water at 70 °C, after which *β*-arbutin was mixed with the extract and the remaining preheated water. The nanoemulsion was stirred for 5 minutes under identical conditions. Moreover, the formulation was subjected to sonication (Elma, Germany) for 30 minutes to removeair bubbles. Moreover, the individual active nanoemulsions, Fe and Fa formulations, were prepared following the same procedure.

Furthermore, the hybrid nanoemulsion was characterized by measuring its pH, transmittance percentage, viscosity, and particle size. The pH was measured in triplicate at room temperature using an automatic pen-type pH meter (Ohaus, USA). The pH of the nanoemulsions was adjusted to be similar to that of human skin, within the range of 4.1–5.8, or close to 6. The transmittance percentage was investigated using a UV–Vis spectrophotometer (Shimadzu, Japan) at a wavelength of 650 nm with purified water as the blank. A transmittance value close to 100% indicates a clear and transparent formulation, reflecting the presence of nanodroplets.

The viscosity of the nanoemulsion was investigated using a viscometer (Rion, Japan) that was configured with rotor spindle No. 3. The adequate viscosity range for nanoemulsion preparations typically falls between 1 and 100 cP. Finally, the distribution and particle size of the nanoemulsions were investigated using dynamic light scattering (DLS) on a Zetasizer Nano ZEN3600 (Malvern Instruments, Malvern, UK). For the analysis, 30 µL of each nanoemulsion sample was diluted in 3 mL of deionized water at room temperature. Particle size was then determined by calculating the Z-average from three independent batches for each nanoemulsion formulation.

In vitro Tyrosinase Inhibition Assay

Various concentrations of *β*-arbutin (0, 80, 160, 240, 320, 400, and 480 ppm) were prepared in assay buffer. Three nano formulations (Fae; Fe and Fa); *β*-arbutin (140 ppm); *Centella asiatica* extract (320 ppm); kojic acid (inhibitor control; IC); and tyrosinase (tyrosinase enzyme control; EC), were each added at 20 µL into a 96-well microplate. Subsequently, tyrosinase enzyme solution (50 µL) was pipetted into each well and incubated for 10 min at 25°C. Then, tyrosinase substrate (30 µL) solution was added after the incubation.[21] The microplate containing the samples, IC, and EC was then measured using a multi-mode reader (Allsheng FlexA-200, China) at 510 nm, with two readings taken between 1 and 20 min. The absorbance values obtained were used to calculate the percentage of relative inhibition (%RI) using the following equation:

$$\%\text{Relative Inhibiton} = \frac{(\text{Slope(EC)} - \text{Slope(S)})}{\text{Slope(EC)}} \times 100\%$$

Where Slope (S) and Slope (EC) were calculated as:

$$\text{Slope} = \frac{\Delta Abs(Abs2 - Abs1)}{\Delta T(T2 - -T1)}$$

In vitro Melanogenesis Inhibition in B16 Melanoma Cells

B16F10 cells were maintained in high-glucose DMEM supplemented with 10% FBS and 1% penicillin-streptomycin at 37°C in a humidified atmosphere containing 5% CO_2. After reaching the confluent level, the cells were harvested using 0.25% trypsin-EDTA. The cells were then cultured at a density of 5.0 x 10^5 cells per well in 6-well plates and incubated in a CO_2 incubator for 24 h. Subsequently, three formulations (Fae; Fe and Fa), *β*-arbutin (140 ppm), kojic acid (140 ppm), and *Centella asiatica* extract (140 ppm) were added and incubated for an additional 72 h. At the end of the incubation period, the cells were washed with PBS, dissolved in 10% NaOH, and incubated at 60ºC for 1 hour (ThermoScientific, USA).[28] The absorbance at 450 nm was measured to quantify the melanin content and calculate the percentage of anti-melanogenesis activity using the following equation:

$$\%\ Anti\ melanogenesis = 100 - [(\frac{Mt}{Mc}) \times 100]$$

Here, M_t is the melanin content in the treated group, while M_c is the melanin content in the untreated control group.

Statistical Analysis

All data were preprocessed to identify outliers. Afterward, the data were presented as means ± standard deviations (SDs) or standard error of the mean from at least three independent measurements. The data were analyzed using one-way Analysis of Variance (ANOVA), with the level of significance determined at $^*p < 0.05$. In this step, we used Microsoft Excel 2019 (Excel Version 17) to perform all calculations.

Results and Discussion

Bioinformatic analysis to predict the gene target of β-arbutin

This study integrated bioinformatics, *in silico*, and *in vitro* approaches to elucidate the mechanism of antimelanogenic activity of a *β*-arbutin and asiaticoside hybrid nanoemulsion. The combination of these two bioactive compounds was designed to investigate their complementary mechanisms. Arbutin, as a hydroquinone glycoside, exhibits antioxidant activity and competitively inhibits tyrosinase,[29] whereas asiaticoside, as a triterpenoid saponin, has been reported to have antioxidant, as well as skin-lightening and antiaging effects.[19,21,30,31,32] The hydrophilic characteristic of arbutin and the lipophilic properties of asiaticoside allow their formulation as a novel delivery method to increase bioaccessibility and stability.[33]

Asiaticoside is a saponin glycoside containing sugar molecules (glucose-glucose-rhamnose) linked to a triterpene group. In contrast, *β*-arbutin is an isomer of arbutin, a compound with a structure in which one D-glucose molecule is bound to hydroquinone (Figure 1a). Based on data mining results, there were 12,727 pigmentation genes identified. These pigmentation genes were intersected with 85 asiaticoside-associated genes and 11 *β*-arbutin-associated genes (Figure 1b). Venn diagram and PPI network analyses revealed three main genes related to asiaticoside, *β*-arbutin, and pigmentation: TYR, MITF, and DCT (Figure 1c). Furthermore, the MCC method was applied to identify the genes or proteins that are most strongly affected by asiaticoside and *β*-arbutin in pigmentation regulation.

Based on the analysis, this study observed that these three genes have comparable levels of significance in skin pigmentation affected by asiaticoside and *β*-arbutin (Figure 1d). TYR functions as the rate-limiting enzyme converting the oxidation of tyrosine to DOPA and subsequently to DOPAquinone, while DCT converts DOPAchrome to DHICA, contributing to eumelanin synthesis.[4,36,37] Meanwhile, MITF serves as a master regulator of melanocyte differentiation and pigmentation by controlling the transcription of TYR, DCT, and other melanogenic genes (Table 1).[38] The interference of asiaticoside and *β*-arbutin with these core genes suggests a dual-level inhibition, involving both direct enzymatic suppression and upstream transcriptional modulation. These findings are consistent with previous studies reporting that the downregulation of MITF and TYR results in reduced

ISSN 2616-0684 (Print)
ISSN 2616-0692 (Electronic)

melanin synthesis in melanocytes, thereby confirming the biological relevance of the predicted targets.

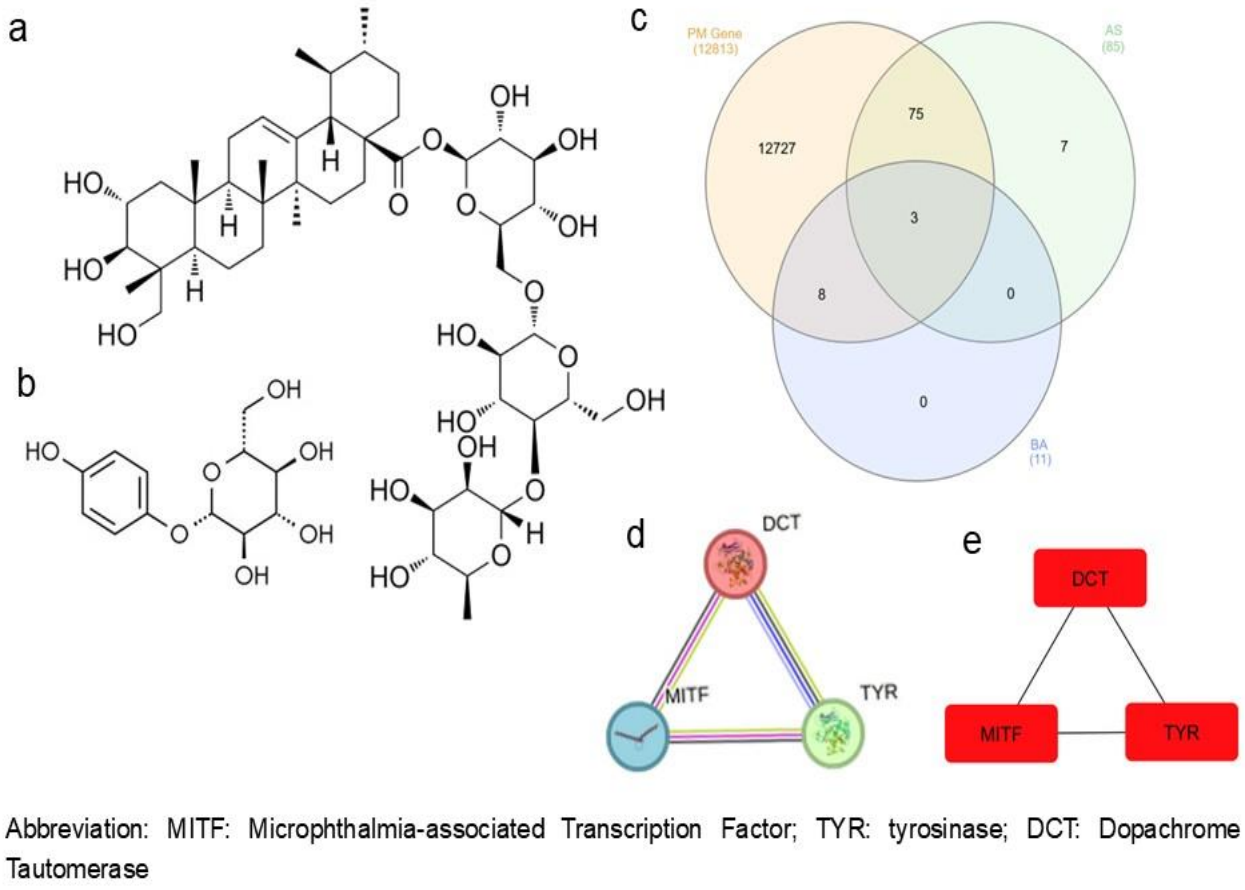

Figure 1: Gene targets analysis of *β*-arbutin and asiaticoside combination on melanogenesis; a. Molecular Structure of *β*-arbutin and asiaticoside, b. Venn diagram of arbutin, asiaticoside, and hyperpigmentation-melanogenesis interfered genes, c. Protein-protein interaction (PPI) network of the intersecting genes; d. The clustering of the interfered genes related to melanogenesis and hyperpigmentation according to MCC.

Table 1: The top three pigmentation-related genes influenced by tyrosinase and their biological functions

No.	Gene symbol	Protein name	Biological Function
1	MITF	Microphthalmia-associated Transcription Factor	A key transcription factor that regulates the expression of melanogenic enzymes, including tyrosinase, by binding to specific DNA sequences in promoter regions.[34, 35]
2	TYR	Tyrosinase	A rate-limiting oxidase enzyme responsible for catalyzing the conversion of tyrosine to melanin precursors within melanosomes.[4]
3	DCT	DOPAChrome Tautomerase	An enzyme that catalyzes the conversion of DOPAchrome to its carboxylated derivative, DHICA, which subsequently polymerizes to eumelanin.[36]

In Silico Molecular Docking

Molecular docking studies were performed to predict the potential binding, thereby providing a fundamental result for further investigation of pigmentation-related genes with asiaticoside and *β*-arbutin. Further, this study also investigated molecular docking analysis of asiaticoside and *β*-arbutin with the MITF and TYR proteins.

Based on the molecular docking analysis, there are molecular bindings between MITF and test compounds (asiaticoside and *β*-arbutin). As shown in Figure 2a and Table 2, there are six amino acid residues forming hydrogen bonds between MITF and asiaticoside, namely Ser478, Ala476, Ser499, Leu[38]9, Glu382, and Arg386. There are also two hydrophobic bonds and nine van der Waals bonds, namely His387 and His383 for the hydrophobic bonds, and Ala496, Asp479, Ala477,

ISSN 2616-0684 (Print)
ISSN 2616-0692 (Electronic)

Leu498, Gln378, Arg370, Lys379, Arg391, and Gly480 for the van der Waals bonds. Furthermore, there are five hydrogen bonds formed between MITF and *β*-arbutin in Lys497, Glu494, Asp431, Leu429, and Arg406, and one hydrophobic bond was identified, which is Ala496 (see Figure 2c and Table 2). The van der Waals bonds formed are Asp479, Ser478, Ala477, Lys493, Gly430, Glu432, His387, Leu390, Gly495, and Arg386. Based on the molecular binding energy values, the MITF and *β*-arbutin complex (-6.23 kcal/mol) exhibited a slightly stronger bond than the MITF and asiaticoside complex (-6.20 kcal/mol).

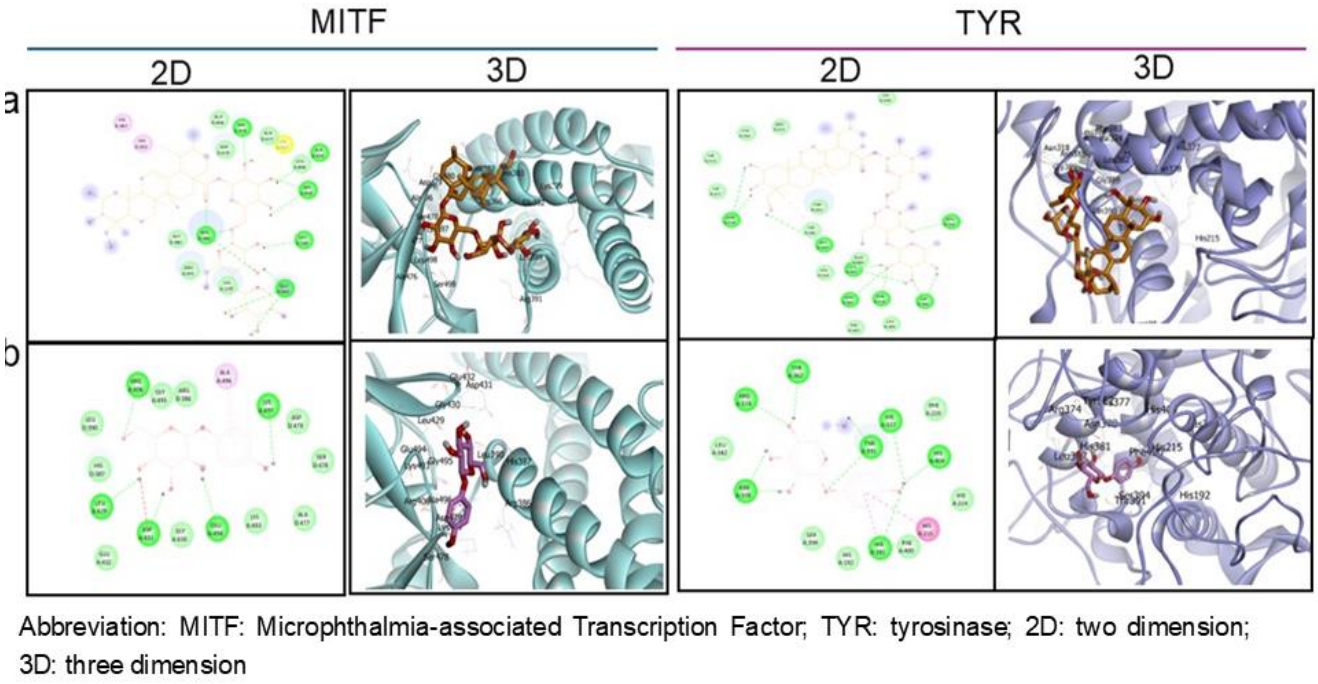

Figure 2: The binding pose derived by molecular docking simulation, both in 2D binding pose (left) and 3D docked pose (right) of the MITF and TYR with asiaticoside (a, b) and arbutin (c,d).

Table 2: Molecular docking results of MITF and TYR with asiaticoside and *β*-Arbutin, showing binding energies and interactions with amino acid residues

Protein Target	Compound	Binding Energy (kcal/mol)	Hydrogen Bond residues	Hydrophobic residues	Van der Waals residues
TYR	*β*-Arbutin	−5.93	His404, His381, Asn378, Arg374, Tyr362, Thr391, His377	His215	His224, Phe400, His192, Ser394, Leu382, Phe220
	Asiaticoside	−6.38	Arg321, Gly386, Asn318, Asn385, Leu382, Gly389, Asn378	Leu382	His377, His215, Val196, Val391, Tyr369, Asn350, Tyr348, Gly389, Gln390
MITF	*β*-Arbutin	−6.23	Lys497, Glu494, Asp431, Leu429, Arg406	Ala496	Asp479, Ser478, Ala477, Lys493, Gly430, Glu432, His387, Leu390, Gly495, Arg386
	Asiaticoside	−6.20	Ser478, Ala476, Ser499, Leu389, Glu382, Arg386	His387, His383	Ala496, Asp479, Ala477, Leu498, Gln378, Arg370, Lys379, Arg391, Gly480

ISSN 2616-0684 (Print)
ISSN 2616-0692 (Electronic)

Apart from MITF, Arg 321, Gly386, Asn318, Asn385, Leu382, Gly389, and Asn378 of TYR formed hydrogen interaction with asiaticoside. Furthermore, there are also seven hydrogen bonds between TYR and *β*-arbutin, namely His404, His381, Asn378, Arg374, Tyr362, Thr391, and His377. There is one hydrophobic bond each between TYR with asiaticoside and with *β*-arbutin through Leu382 and His215, respectively. There are also van der Waals interactions formed, with His377, His215, Val196, Val391, Tyr369, Asn350, Tyr348, Gly389, and Gln390 between TYR with asiaticoside and with *β*-arbutin, TYR, and asiaticoside, while His224, Phe400, His192, Ser394, Leu382, and Phe220 were identified between TYR and *β*-arbutin (Figure 2b and Table 2). Then, when analyzed from the minimum binding energy, the interaction between asiaticoside and TYR (-6.38 kcal/mol) has a better interaction than that between *β*-arbutin and TYR (-5.93 kcal/mol) (Figure 2d, Table 2). These results imply that both compounds can interact with key melanogenic targets, but their binding preferences differ—*β*-arbutin favors MITF, while asiaticoside shows stronger affinity for TYR.

TLC Analysis

This study extracted *Centella asiatica* herbal using 70% ethanol as the solvent, which was then combined with *β*-arbutin as a nanoemulsion. Before the formulation process, we conducted TLC analysis to detect the presence of asiaticoside in the *Centella asiatica* extract, as indicated by the appearance of a red spot on the TLC plate. The sample revealed an R_f value of 0.32, while the standard reference appeared to have an R_f value of 0.31 (Figure 3a). These findings confirm that the *Centella asiatica* extract contains asiaticoside, observed by the red fluorescent spot under UV light at 365 nm, which was identical to that of the reference standard, and the closely comparable R_f value. According to previous studies, *Centella asiatica* extract contained several triterpenoid compounds, including asiaticoside, madecassoside, asiatic acid, and madecassic acid. A second spot, with an R_f value of 0.19, was presumed to correspond to madecassoside. This is supported by literature reporting that madecassoside exhibits an R_f value of approximately 0.16 under the same mobile phase conditions.[19,21] Therefore, spot number 2 was predicted as madecassoside in the *Centella asiatica* extract.

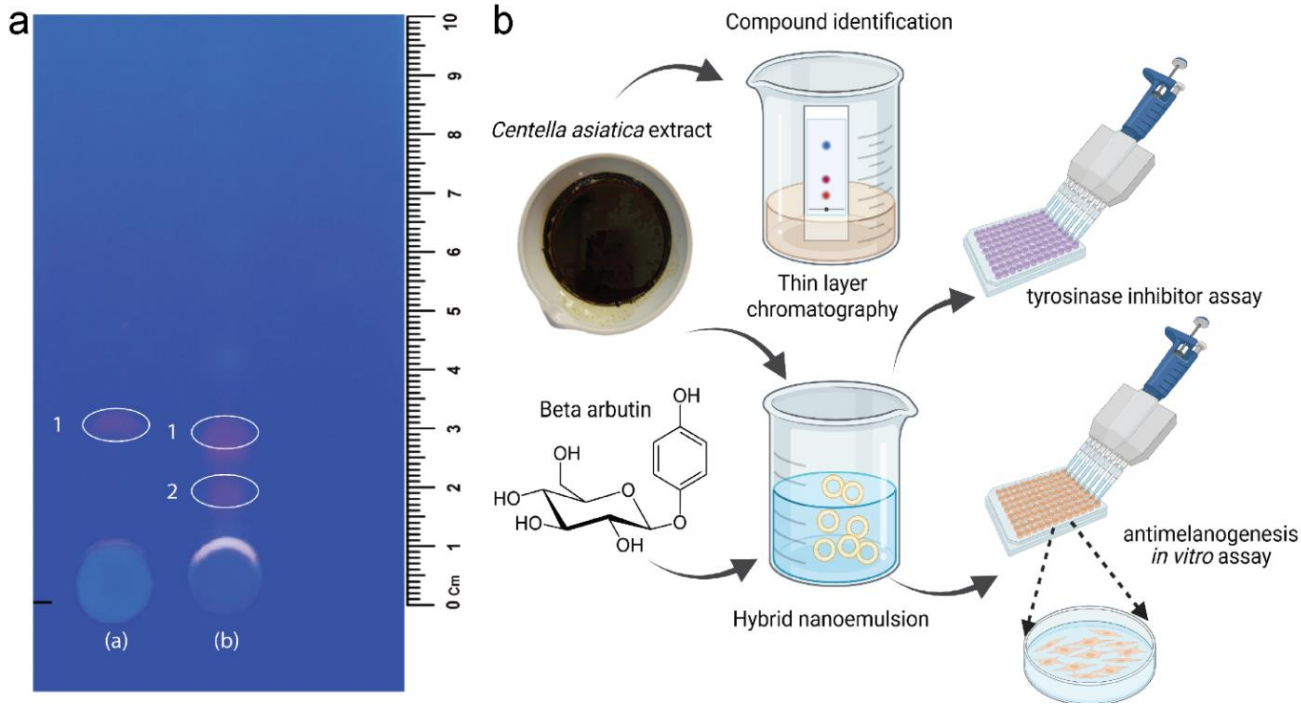

Figure 3: Asiaticoside detection of *Centella asiatica* extract, hybrid formulation, and anti-melanogenesis activity test. a. The thin-layer chromatography (TLC) analysis of *Centella asiatica* extract to detect asiaticoside compound; 1. Asiaticoside, 2. Madecacosside. b. Scheme of hybrid emulsion formulation, and anti-melanogenesis activity test. The scheme was prepared in Biorender.

Hybrid Nanoemulsion Formulation and Its Characterization

This study developed three nanoemulsion formulas – Fa, Fe, and Fae – with each one containing different active components. Fa and Fe contained *β*-arbutin, and the *Centella asiatica* extract, respectively, and Fae is a hybrid nanoemulsion of both active components (Figure 3b). All three formulas produced a similar visual: a yellowish, clear, and homogeneous appearance, reflecting the uniform formation and stable dispersions of the droplets (Figure 4a).

The formulations showed pH values between 4.13 ± 0.057 and 4.27 ± 0.057 (Table 3), which fall in the acceptable range for dermal applications. Since skin naturally maintains a pH range between 4.1 and 5.8, or close to 6, these pH values also suggest minimal potential for skin irritation. Viscosity measurements, however, reveal decreasing values, from Fa (5.07 ± 0.047 cP), Fe (4.07 ± 0.047 cP), to Fae (3.07 ± 0.047 cP) (Table 3). A significant decrease suggests the active materials may have reduced the internal structural resistance of the nanoemulsion matrix.

Moreover, another physical characteristic of nanoemulsion was the transmittance value, which was uniformly high, exceeding 80%, indicating the nanoscale-sized droplet and high optical clarity. Fae shows the highest transmittance of 93.80 ± 0.346% (Table 3) and exhibits its superior droplet uniformity and dispersion stability. To date, these physicochemical characteristics verify the efficacy of the nanoemulsions for delivering the incorporated bioactive actives topically.

ISSN 2616-0684 (Print)
ISSN 2616-0692 (Electronic)

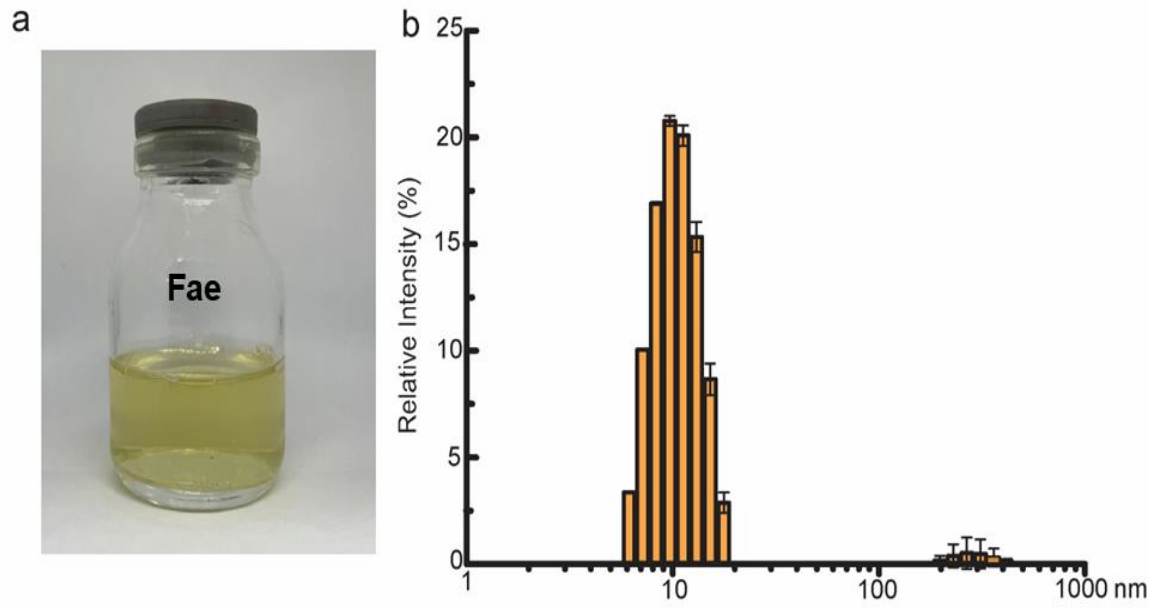

Figure 4: Characteristics of hybrid nanoemulsion. a. Physical appearance of the hybrid nanoemulsion, b. Particle size distribution analysis of the hybrid nanoemulsion using Dynamic Light Scattering (DLS).

Table 3: Physicochemical Characteristics of Nanoemulsion

Parameter	Fa	Fe	Fae
Organoleptic Properties	Yellowish, clear, and homogeneous	Yellowish, clear, and homogeneous	Yellowish, clear, and homogeneous
pH	4.20 ± 0.10	4.13 ± 0.057	4.27 ± 0.057
Viscosity (cP)	5.07 ± 0.047	4.07 ± 0.047	3.07 ± 0.047
Transmittance (%)	90.08 ± 0.125	81.33 ± 0.23	93.80 ± 0.346

Abbreviations Fa = Nanoemulsion Arbutin; Fe = Nanoemulsion *Centella asiatica*; Fae: Nanoemulsion Arbutin with *Centella asiatica;* ± = Standard deviation; cP = centi poise

To ensure the particle's nanoscale size, further measurement was carried out using a Particle Size Analyzer (PSA). The hybrid formulation revealed a z-average of 17.61 ± 0.55 nm, a polydispersity index (PDI) of 10.642 ± 0.019, and a diameter of 10.44 ± 0.284 nm. These values were below the <100 nm size conventionally associated with nanoemulsions, suggesting effective emulsification and consistent interfacial stability of droplets. Moreover, the low PDI value (< 0.2) indicated a narrow particle size distribution, confirming the hybrid nanoemulsion's homogeneity.

In Vitro Tyrosinase Inhibition

The nanoemulsions were then evaluated for their anti-melanogenesis activity through an inhibition assay against tyrosinase enzyme, a rate-limiting step in melanogenesis. All three nanoemulsion formulations outperformed the crude extract and pure *β*-arbutin. Fae showed the highest inhibition at 91.54 ± 0.77%, followed by Fa (86.41 ± 0.89%, $p<0.05$) and Fe (83.85 ± 1.54%, $p<.0.05$). *β*-arbutin, as the positive control, attenuated the enzyme by 76.15 ± 1.54%, significantly higher than the extract's inhibitory effect (69.74 ± 1.18%) (Figure 5a).

The data suggested that the formulation of *β*-arbutin ($p < 0.05$), extract ($p < 0.05$), and both ($p < 0.01$) into nanoemulsions enhances the efficacy of *in vitro* tyrosinase inhibition activity. The active encapsulation into nanoemulsion significantly improves its interaction with the tyrosinase enzyme. Fae's excellent performance suggests that *β*-arbutin and the extract have a synergistic effect to elevate anti-tyrosinase inhibition when they are formulated into a nanoemulsion system.

Melanogenesis Inhibition in Murine Melanoma B16F10 Cells

The anti-melanogenesis assay exhibited differences in tyrosinase inhibition percentage among arbutin, the extract, and their nanoemulsion formulations. Fae (13.08 ± 2.02 %) outperformed Fe (12.32 ± 1.10 %) and *β*-arbutin (10.86 ± 1.32%). The non-formulated extract (8.53 ± 0.93 %) and Fa (8.16 ± 1.12 %) showcased noticeably lower inhibition of melanogenesis. The hybrid nanoemulsion displayed remarkably higher inhibition levels than the *β*-arbutin nanoemulsion ($p < 0.01$), although it did not differ significantly from the extract nanoemulsion. These data stipulate that the nanoemulsion formulations, particularly Fae, strengthen the antimelanogenic activity of the *β*-arbutin formulation.

ISSN 2616-0684 (Print)
ISSN 2616-0692 (Electronic)

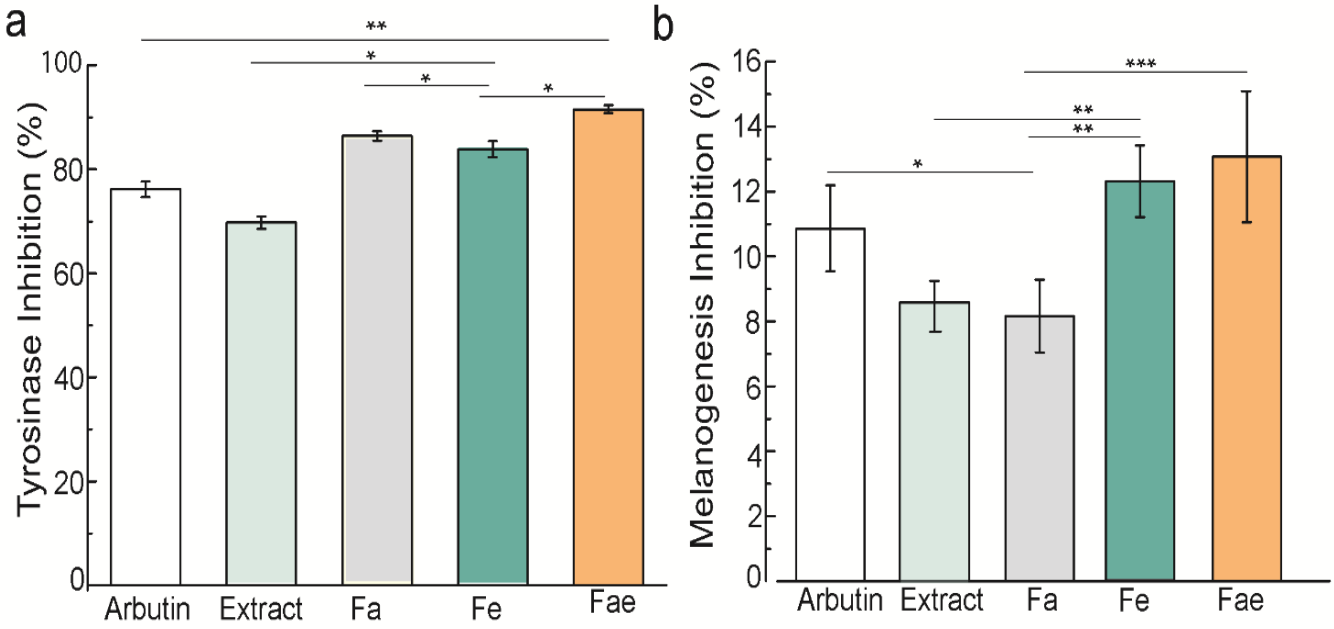

Figure 5: *In vitro* antimelanogenesis activity of *β*-arbutin, extract, single nanoemulsion, and hybrid nanoemulsion. a. Tyrosinase inhibition test; b. Melanogenesis Inhibition in B16 Melanoma Cells. Fa: arbutin nanoemulsion formula, Fe: extract nanoemulsion formula, and Fae: hybrid nanoemulsion formula. *p<0.5, **p<0.01, ***p<0.001.

Both enzyme-based and cell-based assays observed higher tyrosinase inhibition by the formulations than the crude extract or *β*-arbutin itself. This advanced formulation may stem from the better solubility and molecular accessibility of the active compounds to the tyrosinase catalytic site. Co-loading the extract and *β*-arbutin in the nanoemulsion likely contributed to a synergistic effect. Earlier studies suggested the possibility of combining antioxidants with depigmenting agents to modulate multiple melanogenic pathways simultaneously.[15]

The improved anti-melanogenesis effect may also be attributed to enhanced cutaneous penetration and retention. Surfactant-induced disruption of lipid bilayer, reduced droplet size, and increased surface contact assist diffusion through the stratum corneum and deposition within the viable epidermis.[39] Consequently, the active compounds can reach melanocytes efficiently and maintain sustained tyrosinase inhibition. This mechanism is consistent with a previous study describing enhanced delivery of hydrophilic inhibitors (such as *β*-arbutin) and hydrophobic compounds like curcumin through nanoemulsion-based systems, leading to higher antimelanogenic efficacy.[16]

Overall, the strong correlation between *in silico* docking data, *in vitro* enzyme-based, and cell-based assays supports the mechanism for developing nanoemulsions in melanogenesis inhibition activity. Among the formulations, Fae is the most effective for its combined physicochemical advantages, stable binding to the tyrosinase catalytic site in molecular docking, and synergistic bioactive interactions in the cellular melanogenesis assay. This multifaceted focus highlights the potential of nanoemulsion-based systems as advanced carriers for cosmeceutical applications, targeting hyperpigmentation. Nevertheless, further investigations, involving *in vitro* skin permeation and *in vivo* safety evaluations, will be necessary to confirm the translational potential of the developed formulations.

Conclusion

In conclusion, synergistic inhibition of the MITF and TYR pathways was confirmed by the bioinformatics analysis, *in silico* predictions, and *in vitro* validations, which supported the combination strategy. The effective dermal delivery was further supported by the Fae nanoemulsion's physicochemical properties, which included small particle size, high transmittance, and an appropriate pH. To verify the hybrid nanoemulsion's clinical suitability, future research should investigate *in vivo* assessment and gene expression profiling of MITF and TYR in treated cells.

Conflict of Interest

The authors declare no conflict of interest.

Authors' Declaration

The authors hereby declare that the work presented in this article is original and that any liability for

Acknowledgements

This work was supported by the Doctoral Magister scheme of the Internal Research Grant at Sanata Dharma University, grant number No.016/Penel /LPPM-USD/II/2025.

References

1. Hanif N, Al-Shami AMA, Khalid KA, Hadi HA. Plant-based skin lightening agents: A review. J Phytopharm. 2020;9(1):54–60. https://doi.org/10.31254/phyto.2020.9109.
2. Masum MN, Yamauchi K, Mitsunaga T. Tyrosinase inhibitors from natural and synthetic sources as skin-lightening agents. Rev Agric Sci. 2019;(7):41–58. https://doi.org/10.7831/ras.7.41.
3. D'Mello SAN, Finlay GJ, Baguley BC, Askarian-Amiri ME. Signaling pathways in melanogenesis. Int J Mol Sci. 2016;17(7):1–18. https://doi.org/10.3390/ijms17071144.
4. Pillaiyar T, Manickam M, Namasivayam V. Skin whitening agents: Medicinal chemistry perspective of tyrosinase inhibitors. J Enzyme Inhib Med Chem. 2017;32(1):403–25. https://doi.org/10.1080/14756366.2016.1256882.
5. Xu H, Li X, Xin X, Mo L, Zou Y, Zhao G, Yu Y, Chen K. Antityrosinase mechanism and antimelanogenic effect of arbutin esters synthesis catalyzed by whole-cell biocatalyst.

J Agric Food Chem. 2021;69(14):4243–52. https://doi.org/10.1021/acs.jafc.0c07379.
6. Kim HD, Choi H, Abekura F, Park JY, Yang WS, Yang SH, Kim CH. Naturally-occurring tyrosinase inhibitors classified by enzyme kinetics and copper chelation. Int J Mol Sci. 2023;24(9). https://doi.org/10.3390/ijms24098226.
7. Saeedi M, Khezri K, Seyed Zakaryaei A, Mohammadamini H. A comprehensive review of the therapeutic potential of *α*-arbutin. Phytother Res. 2021;35(8):4136–54. https://doi.org/10.1002/ptr.7076.
8. Chakraborty AK, Funasaka Y, Komoto M, Ichihashi M. Effect of arbutin on melanogenic proteins in human melanocytes. Pigment Cell Res. 1998;11(4):206–12. https://doi.org/10.1111/j.1600-0749.1998.tb00731.x.
9. Kai H, Matsuno K. Assessment of the effect of arbutin isomers and kojic acid on melanin production, tyrosinase activity, and tyrosinase expression in B16-4A5 and HMV-II melanoma cells. Planta Med Lett. 2015;2(1):e39–41. https://doi.org/10.1055/s-0035-1557833.
10. Gillbro JM, Olsson MJ. The melanogenesis and mechanisms of skin-lightening agents – existing and new approaches. Int J Cosmet Sci. 2011;33(3):210–21. https://doi.org/10.1111/j.1468-2494.2010.00616.
11. Couteau C, Coiffard L. Overview of skin whitening agents: Drugs and cosmetic products. Cosmetics. 2016;3(3). https://doi.org/10.3390/cosmetics3030027.
12. Avonto C, Wang YH, Avula B, Wang M, Rua D, Khan IA. Comparative studies on the chemical and enzymatic stability of alpha- and beta-arbutin. Int J Cosmet Sci. 2016;38(2):187–93. https://doi.org/10.1111/ics.12275.
19. Kwon KJ, Bae S, Kim K, An IS, Ahn KJ, An S. Asiaticoside, a component of *Centella asiatica*, inhibits melanogenesis in B16F10 mouse melanoma. Mol Med Rep. 2014;10(1):503–7. https://doi.org/10.3892/mmr.2014.2159.
20. Bandopadhyay S, Mandal S, Ghorai M, Jha NK, Kumar M, Radha, Ghosh A, Prockow J, Perez JM, Dey A. Therapeutic properties and pharmacological activities of asiaticoside and madecassoside: A review. J Cell Mol Med. 2023;27(5):593–608. https://doi.org/10.1111/jcmm.17635.
21. Setiawati A, Maharani BA, Sari PAP, Wyantara KA, Saputra BW, Febriansyah R, Dwiastuti R. Deciphering the molecular pathway of an asiaticoside-rich fraction of *Centella asiatica* as an anti-melanogenesis agent. J HerbMed Pharmacol. 2024;13(2):269–79. https://doi.org/10.34172/jhp.2024.49332.
22. Kaci M, Belhaffef A, Meziane S, Dostert G, Menu P, Velot G. Nanoemulsions and topical creams for the safe and effective delivery of lipophilic antioxidant coenzyme Q10. Colloids Surf B Biointerfaces. 2018;167:165–75. https://doi.org/10.1016/j.colsurfb.2018.04.010.
23. Wei R, Wang J, Su M, Jia E, Chen S, Chen T, Ni Y. Missing-Value M-V. In vitro studies. Target Mol Imaging. 2018;13–13. https://doi.org/10.1038/s41598-017-19120-0.
24. Solans C, Izquierdo P, Nolla J, Azemar N, Garcia-Celma MJ. Nano-emulsions. Curr Opin Colloid Interface Sci. 2005;10(3–4):102–10. https://doi.org/10.1016/j.cocis.2005.06.004.
25. Sukarjati,Kusuma PSW,Rahayu A,Ambarwati N,Hardani PT, Badriya L, Puspitasari M, Ikwias LM.Evaluation and Antimicrobial Activity of Herbal Nanoemulgel Combination of N-Butanol Extracts of *Centella asiatica and Sapindus rarakand* Seed Oil of *Azadirachta indica*. Trop J Nat Prod Res. 2024; 8(2):6134-6141. http://www.doi.org/10.26538/tjnpr/v8i2.10.
26. Monton C, Settharaksa S, Luprasong C, Songsak T. An optimization approach of dynamic maceration of *Centella asiatica* to obtain the highest content of four centelloids by response surface methodology. Rev Bras Farmacogn. 2019;29(2):254–61. https://doi.org/10.1016/j.bjp.2019.01.001.
13. Sahudin S, Sahrum Ayumi N, Kaharudin N. Enhancement of skin permeation and penetration of *β*-arbutin fabricated in chitosan nanoparticles as the delivery system. Cosmetics. 2022;9(6):1–14. https://doi.org/10.3390/cosmetics9060114.
14. Tantanasrigul T. The efficacy of a topical cosmetic containing alpha-arbutin 5% and kojic acid. J Cosmet Dermatol. 2024. https://doi.org/10.1111/jocd.16562
15. Siridechakorn I, Pimpa J, Choodej S, Ngamrojanavanich N, Pudhom K. Synergistic impact of arbutin and kaempferol-7-O-*α*-L-rhamnopyranoside from *Nephelium lappaceum* L. on whitening efficacy and stability of cosmetic formulations. Sci Rep. 2023;13(1):1–9. https://doi.org/10.1038/s41598-023-49351-3.
16. Sainakham M, Promma B, Ngernthong A, Kiattisin K, Boonpisuttinant K, Wuttikul K, Jantrawut P, Ruksiriwanich W. Preparation and stability investigation of ultrasound-assisted W/O/W multiple nanoemulsions co-loaded with hydrophobic curcumin and hydrophilic arbutin for tyrosinase inhibition. Heliyon. 2024;10(14):e34665. https://doi.org/10.1016/j.heliyon.2024.e34665.
17. Da Rocha PBR, Souza BS, Andrade LM, Dos Anjos JLV, Mendanha SA, Alonso A. Enhanced asiaticoside skin permeation by *Centella asiatica*-loaded lipid nanoparticles: Effects of extract type and study of stratum corneum lipid dynamics. J Drug Deliv Sci Technol. 2019;50:305–12. https://doi.org/10.1016/j.jddst.2019.01.016.
18. Jiang H, Zhou X, Chen L. Asiaticoside delays senescence and attenuates ROS generation in UV-exposed cells through regulation of TGF-β1/Smad pathway. Exp Ther Med. 2022;24(5):1–13. https://doi.org/0.3892/etm.2022.11603.
27. Lala, R. R, Patel, P. H. Nanoemulsion for Improved Permeability of *Centella asiatica* Extract: Formulation, Ex-Vivo and In-Vivo Evaluation. *International Journal of Pharmaceutical Sciences and Research*. 2019;10(4);1711-1718. http://dx.doi.org/10.13040/IJPSR.0975-8232.10(4).1711-18.
28. Chung S, Lim GJ, Lee JY. Quantitative analysis of melanin content in aa three-dimensional melanoma cell culture.Scientific Reports. 219;(9);780. https://doi.org/10.1038/s41598-018-37055-y.
29. Boo YC. Arbutin as a skin depigmenting agent with antimelanogenic and antioxidant properties. Antioxidants. 2021;10(7):1–22. https://doi.org/10.3390/antiox10071129.
30. Thong-on W, Pathomwichaiwat T, Boonsith S, Koo-amornpattana W, Prathanturarug S. Green extraction optimization of triterpenoid glycoside-enriched extract from *Centella asiatica* (L.) Urban using response surface methodology (RSM). Sci Rep. 2021;11(1):1–11. https://doi.org/10.1038/s41598-021-01602-x.
31. Bylka W, Znajdek-Awizeń P, Studzińska-Sroka E, Brzezińska M. *Centella asiatica* in cosmetology. Postep Dermatol Alergol. 2013; 30(1):46–9. https://doi.org/10.5114/pdia.2013.33378.
32. Kencana MVSA, Widyantara KA, Christian YA, Saputra BW, Setiawati A. Towards a predicted anti-aging molecular targets of asiaticoside based on bioinformatics analysis. Int J Med Biochem. 2025; 8(2):78–88. https://doi.org/10.5114/10.14744/ijmb.2024.26122.
33. Huang H, Belwal T, Liu S, Duan Z, Luo Z. Novel multi-phase nano-emulsion preparation for co-loading hydrophilic arbutin and hydrophobic coumaric acid using hydrocolloids. Food Hydrocoll. 2019; 93:92–101. https://doi.org/10.1016/j.foodhyd.2019.02.023
34. Saeedi M, Eslamifar M, Khezri K. Kojic acid applications in cosmetic and pharmaceutical preparations. Biomed Pharmacother. 2019; 110:582–93. https://doi.org/10.1016/j.biopha.2018.12.006.
35. Desmedt B, Courselle P, De Beer JO, Rogiers V, Grosber M, Deconinck E, et al. Overview of skin whitening agents with an insight into the illegal cosmetic market in Europe. J Eur

ISSN 2616-0684 (Print)
ISSN 2616-0692 (Electronic)

Acad Dermatol Venereol. 2016;30(6):943–50. https://doi.org/10.1111/jdv.13595.
36. Zhou S, Zeng H, Huang J, Lei L, Tong X, Li S. Epigenetic regulation of melanogenesis. Ageing Res Rev. 2021;69. https://doi.org/10.1016/j.arr.2021.101349.
37. Yang CY, Guo Y, Wu WJ, Man MQ, Tu Y, He L. UVB-induced secretion of IL-1β promotes melanogenesis by upregulating TYR/TRP-1 expression in vitro. Biomed Res Int. 2022;2022. https://doi.org/10.1155/2022/8230646.
38. Maddaleno AS, Camargo J, Mitjans M, Vinardell MP. Melanogenesis and melasma treatment. Cosmetics. 2021;8(3):1–1. https://doi.org/10.3390/cosmetics8030082.
39. Ajazuddin, Alexander A, Khichariya A, Gupta S, Patel RJ, Giri TK. Topical analgesics for acute and chronic pain in adults – an overview of Cochrane Reviews. Int J Pharm. 2019;11(11):36–48. https://doi.org/10.1002/14651858.CD008609.pub2.
40. Appendices